Studies on protein transmission in thin channel flow module: the role of dean vortices for improving mass transfer

Jasmedh Kaur, G.P. Agarwal*

Department of Biochemical Engineering and Biotechnology, IIT Delhi, Hauz Khas, New Delhi 110016, India

Received 1 June 2000; accepted 13 March 2001

Abstract

This study is mainly comprised of evaluating mass transfer coefficient from the volumetric flux and protein transmission data in a thin channel flow module. Dilute solutions of lysozyme were ultrafiltered through hydrophilic membrane (cellulose acetate type) with molecular weight cut off (MWCO) of 30,000. Experiments were performed in thin channel flow (TCF10) configuration and data for transmission and volumetric flux obtained as a function of pressure and cross flow velocity. The results were analysed keeping into account the formation of Dean vortices and it was seen that the presence of Dean vortices gave better performance in terms of mass transfer. The mass transfer coefficient obtained with Dean vortices was comparable with the other commercial cross flow system involving secondary flow like Taylor vortices. A new mass transfer correlation has also been presented and compared with the reported correlations in literature.

Keywords: Protein transmission; Thin channel; Ultrafiltration; Dean vortices; Mass transfer coefficient

1. Introduction

Ultrafiltration is being used increasingly as a concentration and separation process as it offers several advantages over the traditional separation methods. However, with the development of high flux membranes and need to filter concentrated solutions, attention has been given to increasing performance through improved mass transfer and fluid mechanics. The limitation on the performance of pressure driven membrane filtration, from inadequate mass transfer and poor fluid mechanics manifests itself through the effects of concentration polarisation and fouling. An increasing effort has been focused on these problems both with the view of understanding and alleviating them. Concentration polarisation results in a localised increase in solute concentration at the membrane surface. The consequence is a decrease in the permeate flux, thus, affecting the performance of filtration operation that represents obstacle to the use of membrane process. To reduce concentration polarisation and fouling, there are various approaches for lowering the concentration gradient between the bulk fluid and the membrane surface and for re-entraining the solids deposit on the membrane surface. These include physical methods like mechanical scouring, chemical methods such as surface modification of the membrane so as to minimise the interactive forces between the deposit and the membrane, hydrodynamic methods such as improved fluid mechanics and module design for reducing solute concentration and

Nomenclature

C_b	protein concentration in the bulk solution (g/l)
C_p	protein concentration in the permeate (g/l)
C_w	protein concentration at the membrane wall (g/l)
C_g	protein gel concentration (g/l)
D	diffusion coefficient (m^2/s)
De	Dean number ($Re\sqrt{d_i/d_c}$)
D_h	equivalent hydraulic diameter
D_∞	free solution Brownian motion diffusivity (m^2/s)
J_v	volummetric flux (m/s)
k	mass transfer coefficient (m/s)
K_d	hindrance factor for diffusive transport
L	channel length (m)
Pe^*	membrane Peclet number based on the bulk mass transfer coefficient $Pe^* = (\tau_a/\varepsilon\phi K_d)(k\delta_m/D_\infty)$
Re	Reynold number based on channel cross flow dimension $Re = (\rho V d_i/\mu)$
Sc	Schmidt number ($=\nu/D$)
Sh	Sherwood number ($=kd_h/D$)
V	average velocity of fluid (m/s)

Greek letters

δ_m	membrane thickness
ε	porosity of membrane
ϕ	equilibrium partition coefficient of solute
ν	kinematic viscosity (m^2/s)
τ	true transmission coefficient
τ_a	the asymptotic value of transmission coefficient attained at infinite Peclet number
τ_{ob}	observed transmission coefficient

deposition on the membrane. Flow instabilities can be useful in overcoming concentration polarisation. Various possibilities include use of eddies during turbulent flow [1], baffles, pulsation [2] rotating membrane filter (Taylor vortex flow) and secondary flow (Dean vortex flow). The use of well ordered Taylor vortices established in a rotating annular filter module is one of the most successful depolarising methods applied in enzyme fractionation, cell harvesting, cell debris removal and even diagnosis of fouling [3–6]. However, any design based on rotating the membrane module will require substantially more energy than stationary systems. So the complexity and scaling difficulties with rotating module systems has limited large-scale commercial development.

An alternate method of establishing centrifugal vortices resulting from the onset of unstable flow in spiral wound membrane ducts has been investigated by Chung et al. [7,8]. Such Dean vortex flow has similar advantage, as Taylor vortex flow but is also amenable to scale up. In addition, it is not expected to consume unreasonable amounts of energy nor have scaling difficulties. At sufficiently low flow rates (as measured by Reynolds number) the velocity in the curved channel flow is approximately stream wise parabolic. However, at Reynold number (or Dean number) above a critical value, centrifugal instabilities cause secondary flow containing streamwise oriented Dean vortices similar to Taylor vortices. These vortices enhance back migration through convective flow away from the membrane solution interface, depolarising the solute build up near the membrane solution interface allowing for increased membrane permeation rates [9–11].

The usefulness of this technique has already been shown in the case of gas–liquid contactors for blood oxygenation [12] and the presence of vortices gives an improvement in oxygen transfer of a factor of 2–4 [13]. The present paper deals with methods of inducing instabilities as a result of Dean vortices. A thin channel (TC) flow module was evaluated experimentally in terms of its mass transfer coefficient. The work reported here has the objective of demonstrating that Dean vortices emanating from sufficient flow around a curved channel indeed result in improved mass transfer at the membrane surface. To our knowledge, this is the first paper to study mass transfer coefficient evaluated from transmission data for this module, although this module has been in use for the last two decades.

2. Theory

The secondary flows, which appear in a curved channel, are due to the difference in pressure between the internal and the external wall of the channel (centrifugal force). At sufficiently small Reynold number,

the velocity in curved channel flow is purely streamwise. Its profile is similar to the parabolic profile of plane channel flow, but the location of maximum velocity is shifted towards the outer wall. This flow is called curved channel Poiseuille flow (CCPF). At higher Reynold number, the centrifugal force pushes fluid elements radially outwards. To maintain the continuity of mass, an equal amount of fluid elements move inwards in reverse radial direction. At a particular flow rate called critical Dean number, the centrifugal instabilities causes a secondary flow containing streamwise-oriented Dean vortices similar to Taylor vortices of Taylor Couette flow. Dean [14] studied the complex flow pattern in a curved pipe using a concentric toroidal co-ordinate system. Brewster et al. [15] confirmed the existence of a critical Reynold number (Re_c) experimentally, above which steady Dean vortices develop. Dean vortices occur in regularly spaced counter — rotating pairs. The CCPF occurs for $Re < Re_c$, and Dean vortices occur for $Re > Re_c$. Sparrow [16] and Walowit et al. [17] confirmed the value of Re_c found experimentally by Brewster by examining the linear neutral stability of Dean vortices. Dean number is a dynamic parameter governing fluid motion in such a configuration and is defined as

$$De = Re\sqrt{\frac{d_i}{d_c}}$$

where Re is the Reynolds number, 'd_i' the hydraulic diameter and 'd_c' the equivalent centreline diameter of curved channel. The critical Dean's number is a function of the curvature and radius ratio r_i/r_0. In our system (Fig. 1) used here in this study, the channel spacing is constant but radius ratio $\eta = (r_i/r_0)$ is varying. To calculate 'd_c' (the equivalent average centreline diameter), we determined the average diameter as the diameter of the channel is varying. Considering linear variation of radius with respect to angle 'θ' (θ varies from 0 to 6π, since the channel consists of three spirals), we calculated average radius as follows

$$De_{av} = \frac{\int_0^{6\pi} Re\sqrt{\frac{r_i}{r_c}}\,d\theta}{\int_0^{6\pi} d\theta} = \frac{Re\sqrt{r_i}\int_0^{6\pi}\frac{1}{\sqrt{r_0+a\theta}}}{\int_0^{6\pi} d\theta}$$

where r_0 is the initial radius of innermost spiral which is equal to 1.0 cm and 'a' was calculated to be 0.173 from our module geometry.

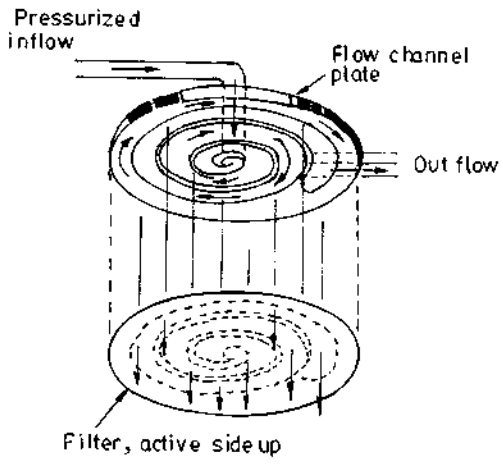

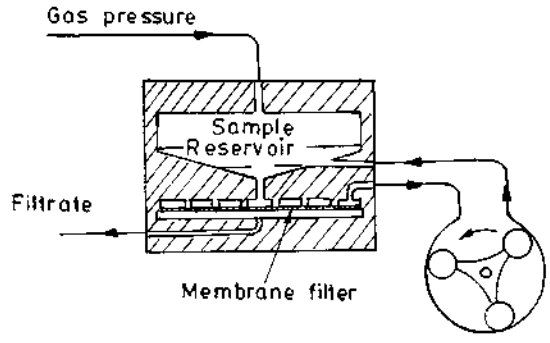

Fig. 1. Two sketches of thin channel flow unit (TCF10) from Amicon. Recirculation of process stream through spiral channel is shown.

Since

$$De_{av} = Re\sqrt{\frac{r_i}{r_{av}}}$$

So

$$Re\sqrt{\frac{r_i}{r_{av}}} = \frac{Re\sqrt{r_i}\int_0^{6\pi}\frac{1}{\sqrt{r_0+a\theta}}\,d\theta}{\int_0^{6\pi} d\theta}$$

By solving this equation, we obtained r_{av} equal to 2.23 cm and hence d_c equal to 4.46 cm.

Similarly 'd_i' was calculated by converting flat rectangular channel into circular channel and calculating the equivalent diameter as

$$d_i = 4\frac{\text{Area}}{\text{Perimeter}} = \frac{4(0.04 \times 0.975)}{2(0.975) + 0.04} = 0.077\,\text{cm}$$

One of the critical elements in such type of centrifugal forces is to predict when the vortex (Dean) formation occurs. This has been done by Brewster et al. [15] who mathematically calculated critical Reynold number as a function of radius ratio (η). It was shown that Re_c was constant ($\cong$33) as η varies from 0.20 to 0.63 and Re_c was between 33 and 45 as η varied from 0.63 to 0.82. In our system, η varies from 0.50 to 0.75 and so Re_c can be assumed to vary between these two extreme values (33–45). Since we always operated experimentally above this range of Reynold number, the formation of Dean vortices was ensured.

3. Materials and methods

3.1. Module and materials

All experiments were carried out using thin channel filter TCF 10 from Amicon USA. It consists of a vessel (reservoir) of 1.5 l capacity, which is always pressurised under operating conditions. From the vessel, the protein solution was circulated by peristaltic pump in the range 50–250 ml/min and the retentate was recycled to the feed tank. The solution moves in a very thin spiral channel over the membrane. In the system, the channel spacing is constant and is 1.0 cm but the radius of the channel is varying as shown in the Fig. 1. The channel consists of three spirals of varying radii from 1.0 to 4.1 cm. Membrane with molecular weight cut off (MWCO) of 30,000 designated as YM30 with filtration area of 40 cm^2 procured from Amicon was used. This membrane is hydrophilic membrane (cellulose acetate type) with exceptionally low nonspecific protein binding properties. Protein solution in TCF 10 module was circulated by peristaltic pump (Watson Marlow 502S) in the range 50–250 ml/min.

Experiments were carried out using lysozyme with Sigma Catalogue No. L-6876. All experiments were done using lysozyme (0.1 g/l) prepared in citric — phosphate buffer. The buffer used throughout the experiments was 0.1 M citric — phosphate buffer and 0.15 M NaCl, pH 6.8. The protein solutions were prepared by dissolving weighed amounts of proteins in buffer and filtered through the sintered glass funnel (G1 grade) to remove any trace colloidal impurities. Citric acid, disodium hydrogen orthophosphate and sodium chloride were of AR grade procured from Qualigens (India).

3.2. Methods

3.2.1. Experimental conditions

All experiments were performed with TCF 10, the schematic diagram of which is shown in Fig. 1. The membrane was equilibrated with protein solutions for 30 min before starting the run. A sample of about 4 ml was taken from the permeate stream to measure the protein concentration. The volummetric flux was measured by timing the known volume using a stopwatch. The protein concentration was measured using UV light at 280 nm.

The volummetric flux and protein concentration was measured as a function of cross flow velocity through the channel and trans membrane pressure (TMP) across the membrane. The reactor vessel was pressurised using nitrogen gas and membrane pressure was measured using manometer (filled with Mercury) connected to feed vessel. The pressure was varied from 10 to 120 kPa. The volummetric flux and permeate concentration was measured until the steady state was reached in $<$5 min. Bulk protein concentration was also measured in feed tank for all pressures. Before the start of each experiment, the buffer flux was measured in the feed vessel for all pressure for which protein solution flux was measured and membrane permeability was calculated. After experimental run with protein solution, the buffer flux was measured again and permeability calculated to assess the membrane fouling. For most of the experiments, fouling was almost non-existence and no appreciable decrease in permeability of membrane was observed. All studies were conducted at a temperature of 25 $\pm$ 1°C.

3.2.2. Mass transfer coefficients

Mass transfer coefficient was calculated using concentration polarisation Eq. (1) as described by Agarwal [18].

$$\ln\left(\frac{\tau_{ob}}{1-\tau_{ob}}\right) = \ln\left(\frac{\tau}{1-\tau}\right) + \frac{j_v}{k}, \quad \text{provided } 0 < \tau < 1 \text{ and } 0 < \tau_{ob} < 1 \tag{1}$$

where

$$\tau = \frac{C_p}{C_w}, \text{ and } \tau_{ob} = \frac{C_p}{C_b}$$

Table 1
Comparison of mass transfer correlations in laminar and turbulent regimes

Ref.	Correlation	Re Range
Lèvêque [27]	$Sh = 1.62(Re\, d_e/L)^{0.33}\, Sc^{0.33}$	Laminar water inside
Jonsson and Boesen [28]	$Sh = 0.04\, Re^{0.75}\, Sc^{0.33}$	Turbulent water inside
Cussler [29]	$Sh = 0.026\, Re^{0.8}\, Sc^{0.33}$	Turbulent water inside
Moulin et al. [13]	$Sh = 0.14\, Re^{0.75}(d_i/d_s)^{0.38}\, Sc^{0.33}$	Laminar water inside
Agarwal [18]	$Sh = 0.29\, Ta^{0.66}\, Sc^{1/3}$	Taylor vortices
	$Sh = 0.25\, Ta^{69}\, Sc^{1/3}$	Taylor vortices
This study	$Sh = 2.80\, De^{0.4}\, Sc^{0.33}$	Laminar

so to use Eq. (1), we need to know either 'k' or concentration of solute at the surface of membrane C_w. Since it is not possible to measure C_w directly, 'k' is estimated from many correlations available in literature. In cross flow filtration, mass transfer coefficient in the form of Sherwood number (Sh) is correlated to Reynold number (Re) and Schmidt number (Sc). For a curved channel flow only one or two correlations are available where Reynold number is replaced by Dean number (De). These correlations are in the form $Sh = A(De)^{\alpha}(Sc)^{1/3}$, the values of constants 'A' and 'α' estimated by various authors are listed in Table 1.

4. Results

This study comprised the analysis of (i) volummetric flux (of both buffer and protein solution) and (ii) protein transmission as a function of trans membrane pressure and cross flow velocity. The volummetric flux (J_v) as a function of trans membrane pressures for different cross flow velocity for buffer solution and protein solution are shown in Fig. 2. It was seen that the protein solution flux matched well with the buffer flux in a range of pressure at all cross flow speeds. At the lowest speed (●) 0.219 m/s; (+) 0.356 m/s; the TMP range where J_v was found to be linear function of

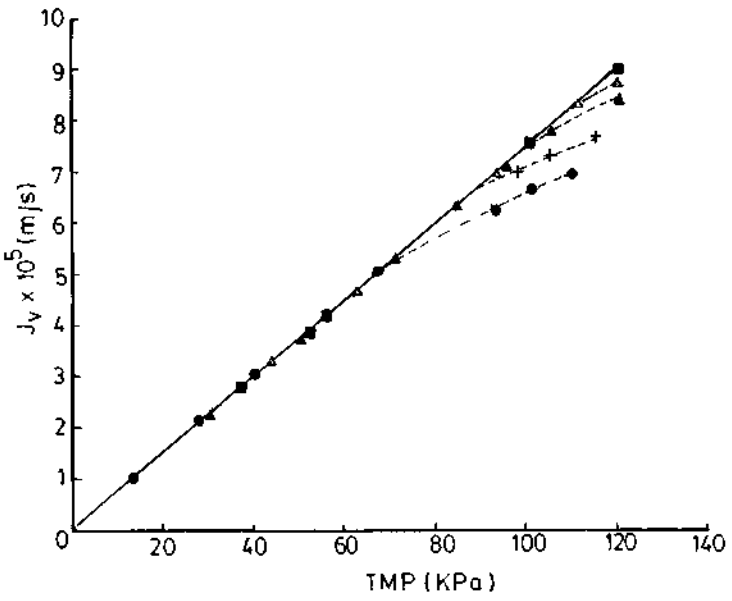

Fig. 2. Volummetric flux vs. TMP for YM-30 membrane at different cross flow velocities for lysozyme solution. (●) 0.219 and 0.356 m/s; (▲) 0.487 m/s; (△) 0.68 m/s; (■) 0.877 m/s. Bold line is for buffer flux.

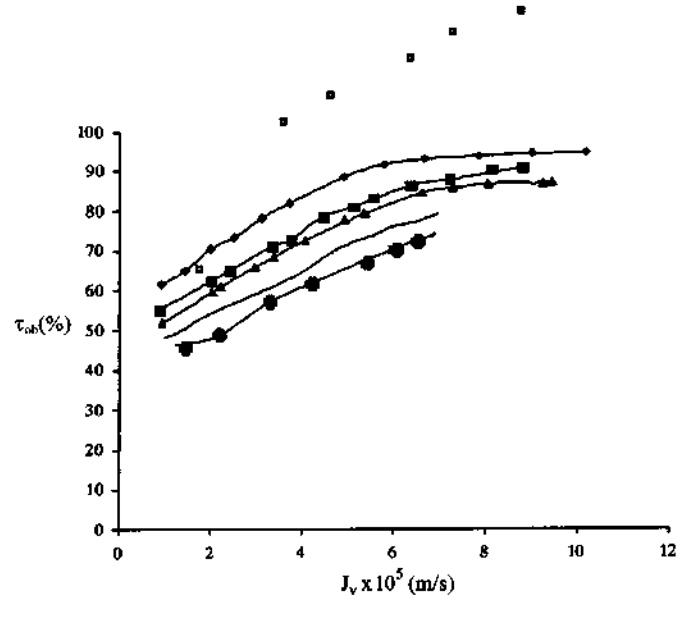

Fig. 3. The observed transmission coefficient (τ_{ob}) vs. volummetric flux (J_v) at different cross flow velocities for lysozyme solution. (◆) 0.219 m/s; (■) 0.356 m/s; (▲) 0.487 m/s; (□) 0.68 m/s and (●) 0.877 m/s.

pressure was 10–85 kPa and increased to 10–120 kPa at the highest speed (0.877 m/s). The corresponding observed protein transmission coefficient (τ_{ob}) data were plotted as a function of J_v at different pump speeds in Fig. 3. The J_v and τ_{ob} were measured for a pressure range of 10–120 kPa. From Fig. 3, it is clear that τ_{ob} increases with increase in J_v for all cross flow velocities. For calculating the mass transfer coefficients using Eq. (1), data for high flux range for low cross flow velocities were screened out to get good fit to Eq. (1) and the reasons for this screening are described by Agarwal [18]. According to this equation, plot between $\ln(\tau_{ob}/1-\tau_{ob})$ and J_v should give straight line with intercept equal to $\ln(\tau/1-\tau)$ and slope equal to '$1/k$' provided 'τ' and 'k' remain constant. Fig. 4 shows good straight lines for all cross flow velocities indicating constant 'k' values with slopes inversely proportional to mass transfer coefficient 'k'. This method of determining mass transfer coefficient is more reliable than other commonly used methods. The procedures commonly employed to determine mass transfer coefficient 'k' in the boundary layer directly from experimental data have been reviewed by van den Berg et al. [20]. However, these methods become questionable because of variation in mass transfer coefficient with changing experimental conditions. Holeschovsky and Cooney [21] used CP model to calculate mass transfer coefficient. In this method, pressure independent volummetric flux, J_v was analysed and high concentration of protein solution (BSA concentration from 10–200 g/l) ensured pressure independent region at relatively low pressures. But our approach here is different because all the experiments were done with very dilute protein solution ensuring that the concentration build up at the surface of the membrane (C_m) is not very high and hence the assumption that diffusivity is independent of concentration is satisfied. Pradanos et al. [22] used same equation (Eq. (1)) to calculate the mass transfer coefficient for a cross flow UF system, but again data analysed for the calculations was that of high pressure condition that give J_v values almost independent of pressure. Here, τ_{ob} changes very slowly and all the data points considered for analysis did lie within just 3–4% variation of transmission, whereas in our analysis transmission varied from 40–90% for the data points considered for calculating mass transfer coefficient. Moreover, the constancy aspect of 'k' was not discussed and is doubtful according to the argument given by Holeschovsky and Cooney [21].

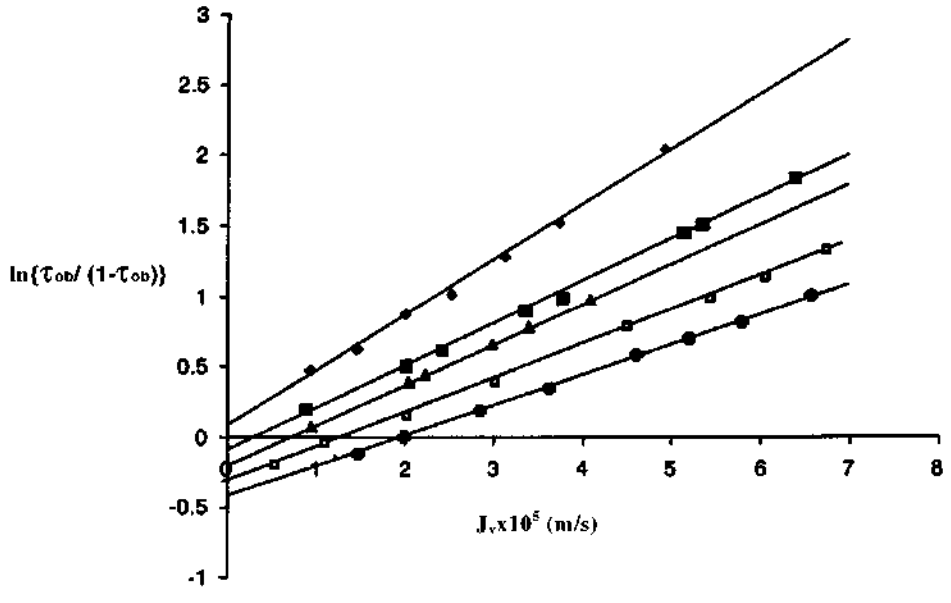

Fig. 4. $\ln\{\tau_{ob}/(1-\tau_{ob})\}$ vs. J_v at different cross flow velocities for lysozyme solution. (◆) 0.219 m/s; (■) 0.356 m/s; (▲) 0.487 m/s; (□) 0.68 m/s; (●) 0.877 m/s.

Fig. 4 also shows that all the lines do not converge to the same point as J_v approaches zero. This means true transmission coefficient 'τ' of the membrane is not constant as expected according to Eq. (1). Actually this transmission coefficient (τ) has been determined from permeate concentration measurements using concentration polarisation (CP) model to account for bulk mass transport effects. Here, we have taken into account only the convective transport contribution to the overall protein flux neglecting the diffusion contribution. But the overall rate of solute transport through the membrane is given by the sum of the diffusive and convective contributions. So 'τ' obtained here at even the highest cross flow velocity may be more than the actual 'τ_a' due to effects of solute diffusion. The actual 'τ_a' is the asymptotic value of transmission coefficient attained at infinite Peclet number (Pe^*), i.e. when the solute transport is totally convective. Increasing the bulk mass transfer coefficient 'k' would decrease 'τ', eventually approaching 'τ_a' as $k \to \infty$, due to reduction in solute diffusion relative to convection. So 'k' has to be very large, which was not obtained in our system in the range of cross flow velocities studied. The true transmission coefficient (τ) is actually related to Pe^* and actual transmission coefficient (τ_a) [19].

$$\tau = \frac{\tau_a(1+Pe^*)}{\tau_a + Pe^*} \tag{2}$$

$$Pe^* = \left(\frac{\tau_a}{\varepsilon\phi K_d}\right)\left(\frac{k\delta_m}{D_\infty}\right) \tag{3}$$

So from Eq. (2), $\tau \to \tau_a$ only if $Pe^* \gg 1$. This condition is relatively easy to satisfy with most track etched membranes since ε is very small ($<0.01\,\mu m$) and δ_m is of the order of $10\,\mu m$. However, the situation is different for asymmetric membranes due to large porosity and very small skin thickness ($\delta_m = 0.5\,\mu m$), so here the τ_a can be estimated from Eq. (3), i.e.

$$\frac{Pe^*}{\tau_a k} = \frac{\delta_m}{\varepsilon\phi K_d D_\infty} = \text{constant} = C \tag{4}$$

Rearranging Eq. (2)

$$\frac{1-\tau}{\tau/\tau_a - 1} = Pe^* \tag{5}$$

Putting Eq. (4) in Eq. (5), we get

$$\frac{1-\tau}{(\tau-\tau_a)k} = C$$

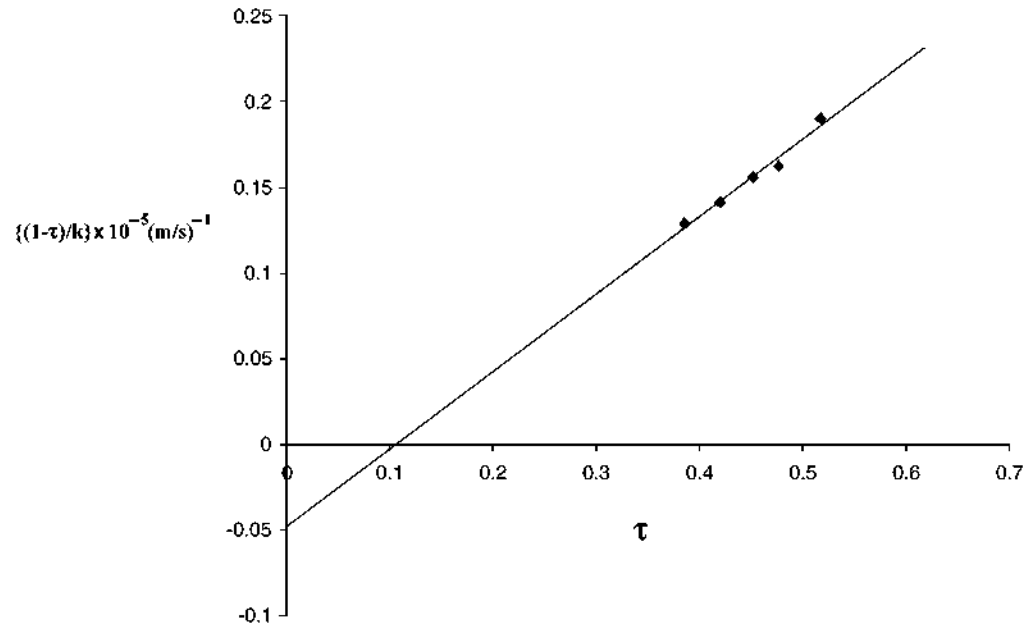

Fig. 5. Determination of the actual transmission coefficient (τ_a) by plotting $(1-\tau)/k$ vs. τ at each cross flow velocity.

or,

$$\frac{1-\tau}{k} = C\tau - C\tau_a \tag{6}$$

Plotting $(1-\tau)/k$ versus τ (Eq. (6)) at each cross flow velocity, will give the actual transmission coefficient (τ_a). As is clear in Fig. 5, we got a straight line and calculated 'τ_a' was found to be 0.11. This 'τ_a' according to Mechanistic Model of solute transport [23] should be equal to the fraction of non-retentive pores of the membrane. For a 30,000 MWCO membrane and lysozyme (MW 13800) system, τ_a (0.11) means that only 11% of the pores transmit lysozyme through 30,000 MWCO membrane, which reflects poorly for the MWCO definition of the membrane. Thus, characterisation of a membrane protein system with respect to 'τ_a' could be a better description of the membrane than mere MWCO which is dependent on the condition of operation due to concentration polarisation.

5. Discussion

The mass transfer coefficients calculated from our experiments fall in the range $(2.5–4.5)\times 10^{-5}$ m/s. The mass transfer coefficients were comparable with the mass transfer coefficients range $(0.4–4.0)\times 10^{-5}$ m/s obtained in case of vortex flow ultrafilter involving Taylor vortices as reported by Agarwal [18].

This implies that the mass transfer coefficient has improved like in the case of Taylor vortices, which are known to be effective in minimising concentration polarisation. This improvement is due to the presence of secondary flows that facilitates mass transfer in the liquid phase. The data give the correlation

$$Sh = 2.80\, De^{0.40}\, Sc^{0.33} \tag{7}$$

With Re in the range of 180–740. The 0.40 dependence of 'De' was found by plotting $(\ln k_{av})$ versus $(\ln Re)$ as shown in Fig. 6. The slope of this graph determines the value of α (0.40). This α value shows a lesser influence of flow on mass transfer than in Taylor vortices (Table 1). The value of 'A' (2.80) was found from the intercept of this graph as given below.

From Eq. (7) it is clear that for a constant Reynold number, the mass transfer coefficient 'k' (included in 'Sh' number) is a function of diameter (d_c) of the channel (included in 'De' number). Since the

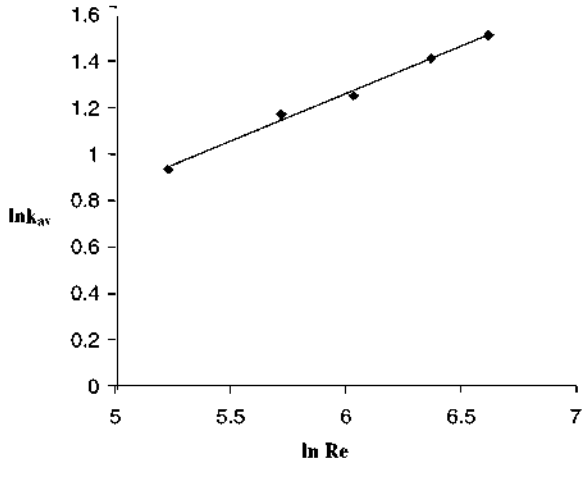

Fig. 6. Mass transfer coefficient ($\ln k_{av}$) vs. Reynold number ($\ln Re$) for lysozyme solution.

diameter of the spiral channel is changing, the mass transfer coeffiecient will also change. The general correlation available in [30] for finding mass transfer coefficient is

$$Sh = A\,De^{\alpha}\,Sc^{\beta} \tag{8}$$

where 'k' in the form of Sherwood number (Sh) is correlated to Reynold (Re) and Schmidt (Sc) numbers. Since $Sh = kd_h/D$

So

$$k = \frac{AD}{d_h} De^{\alpha}\,Sc^{\beta}$$

Here, 'k' is the local mass transfer coefficient, which is function of diameter of the channel. But experimentally we could determine only the average mass transfer coefficient, since it was not possible to determine 'k' at different locations in the channel. Theoretically, this average mass transfer coefficient (k_{av}) can be determined as follows

$$\frac{\int_0^{6\pi} A\,D/d_h\,De^{\alpha}\,Sc^{\beta}\,\mathrm{d}\theta}{\int_0^{6\pi}\mathrm{d}\theta} = \frac{\int_0^{6\pi} A\,D/d_h\,Re^{\alpha}(r_i/r_c)^{\alpha/2}\,Sc^{\beta}\,\mathrm{d}\theta}{\int_0^{6\pi}\mathrm{d}\theta} = A\,D/d_h\,Re^{\alpha}\,r_i^{\alpha/2}\,Sc^{\beta}\,\frac{\int_0^{6\pi}(r_0+a\theta)^{-\alpha/2}\,\mathrm{d}\theta}{\int_0^{6\pi}\mathrm{d}\theta}$$

After integrating and putting the value of limits

$$k_{av} = \frac{2}{(2-\alpha)a\times 6\pi} A\,D/d_h\,r_i^{\alpha/2}\,Sc^{\beta}\,Re^{\alpha} \times\{(r_0+6\pi a)^{1-\alpha/2} - (r_0)^{1-\alpha/2}\}$$

All the constant terms can be lumped together into one parameter (A')

$$k_{av} = A'Re^{\alpha}$$

Or

$$\ln k_{av} = \ln A' + \alpha \ln Re \tag{9}$$

where

$$A' = \frac{2}{(2-\alpha)a\times 6\pi} A\,D/d_h\,r_i^{\alpha/2}\,Sc^{\beta} \times\{(r_0+6\pi a)^{1-\alpha/2} - (r_0)^{1-\alpha/2}\} \tag{10}$$

So by plotting $\ln k_{av}$ versus $\ln Re$ (Fig. 6), the slope determined the value of α and the intercept the value of ($\ln A'$). Putting the values of all parameters, i.e. $r_i = 0.077$ cm, $(r_0 + 6\pi a) = 4.1$ cm, $r_0 = 1.0$ cm, $\alpha = 0.40$ in Eq. (10), the value of 'A' was determined to be 2.80 giving the correlation defined in Eq. (7).

In literature, there are not many correlations available in such type of configuration (spiral). In heat transfer, Mori and Nakayama [24,25] proposed a correlation for coiled tubes that was confirmed by Dravid et al. [26]. In this correlation, a variation with $De^{0.5}$ appears. In mass transfer, the data of Tanishita et al. [12] and Moulin et al. [13] fitted into correlation where variation with $De^{0.75}$ appeared in coiled tubular membranes. If we compare the mass transfer obtained from our correlation with correlations for straight tubes (Table 1), it can be pointed out that the spiral geometry gives better mass transfer than the straight geometry. The mass transfer coefficient has improved by a factor 7–10. The correlation obtained by Jonsson and Boesen [28] and Cussler [29] concern the turbulent regime, whereas in this study with Re between 180 and 740, the flow stayed laminar. So, in the laminar flow, with this geometry, a mass transfer coefficient was measured that is close to the value for turbulent flow in straight channel.

To our knowledge, this is the first paper to study the mass transfer coefficient in thin channel spiral filter evaluated from transmission data.

6. Conclusions

In this work, an ultrafiltration characteristic of single protein (lysozyme) was investigated in TCF10 using hydrophilic 30 kD membrane. The main objective was to establish reliable method to determine mass transfer coefficient for this module and true transmission coefficient of the membrane. Experimental data for lysozyme transmission as a function of filtrate flux for different cross flow velocities were obtained using TCF, with the effects of concentration polarisation evaluated from stagnant film model. The main inferences drawn from this research are as follows:

1. The experimental results were found to be consistent with concentration polarisation (CP) model.
2. This is a better method of characterisation of membranes with respect to true transmission coefficient as it gives a unique value for a protein membrane system depending upon the membrane characteristics and it takes into account the concentration polarisation on the membrane.
3. The more reliable method for determination of mass transfer coefficient is that of evaluation of observed transmission at varying velocity as done here. Both osmotic pressure method and velocity variation methods are not reliable, the former method being very insensitive to changing parameters and the latter rather very sensitive to chosen values of experimental parameters.
4. The 'k' values were quite high ($25–45 \times 10^{-6}$ m/s) as compared to other commercial cross flow systems. This could be attributed to the presence of Dean vortices in this system (thin spiral channel), which are effective in minimising concentration polarisation due to improved mass transfer at the membrane surface. This could be very attractive commercially as it produces vortices without moving the membrane or the module.

Acknowledgements

The financial support to carry the work by IFCPAR Project No. 1615-1 is gratefully acknowledged. G.P. Agarwal acknowledges the discussion on Dean vortices with Dr. P. Aptel and his group during his visit to France. The authors also acknowledge very useful discussions with Dr. P. Aimar and Rajiv K. Thakur while writing the paper.

References

[1] G. Belfort, Fluid mechanics in membrane filtration: recent developments, J. Membr. Sci. 40 (1989) 123.
[2] Y. Wang, J.A. Howell, R.W. Field, D. Wu, Simulation of cross flow filtration for baffled tubular channels and pulsatile flow, J. Membr. Sci. 95 (1994) 243.
[3] K.H. Kroner, V. Nissinen, H. Ziegler, Improved dynamic filtration of microbial suspensions, Biotechnology 5 (1987) 921.
[4] K.H. Kroner, V. Nissinen, Dynamic filtration of microbial suspensions using an axially rotating filter, J. Membr. Sci. 36 (1988) 85.
[5] G. Belfort, J.M. Pimbley, A. Greiner, K-Y. Chung, Dignosis of membrane fouling using rotating annular filter 1. Cell culture media, J. Membr. Sci. 77 (1993) 1.
[6] G. Belfort, P. Mikulasek, J.M. Pimbley, K-Y. Chung, Diagnosis of membrane fouling using a rotating annular filter. 2. Dilute particle suspensions of known particle size, J. Membr. Sci. 77 (1993) 23.
[7] K-Y. Chung, R. Bates, G. Belfort, Dean vortices with wall flux in a curved channel membrane system. 4. Effect of vortices on permeation fluxes of suspensions in microporous membrane, J. Membr. Sci. 81 (1993) 139.
[8] K-Y. Chung, W.A. Edelstein, G. Belfort, Dean vortices with wall flux in a curved channel membrane system. 6. Two dimensional magnetic resonance imaging of the velocity field in a curved impermeable slit, J. Membr. Sci. 81 (1993) 151.
[9] P. Manno, P. Moulin, J.C. Rouch, M. Clifton, P. Aptel, Mass transfer improvement in helically wound hollow fibre ultrafiltration modules yeast suspensions, Separation Purification Technol. 14 (1998) 175.
[10] C. Guigui, P. Manno, P. Moulin, M. Clifton, J.C. Rouch, P. Aptel, J.M. Laine, The use of Dean vortices in coiled hollow fibre ultrafiltration membranes for water and waste water treatment, Desalination 118 (1998) 73.
[11] P. Moulin, P. Manno, J.C. Rouch, C. Serra, M.J. Clifton, P. Aptel, Flux improvement by Dean vortices: ultrafiltration of colloidal suspensions and macromolecular solutions, J. Membr. Sci. 156 (1999) 109.
[12] K. Tanishita, P.D. Richardson, P.M. Galletti, Tightly wound coilds of microporous tubing: progress with secondary-flow blood oxygenator design, Trans Am. Soc. Artif. Int. Organs 21 (1975) 216.
[13] P. Moulin, J.C. Rouch, C. Serra, M.J. Clifton, P. Aptel, Mass transfer improvement in secondary flows: Dean vortices in coiled tubular membranes, J. Membr. Sci. 144 (1996) 235.
[14] W.R. Dean, The streamline motion of fluid in a curved pipe, Philos. Mag. 5 (1928) 674.
[15] D.B. Brewster, P. Grosberg, A.H. Nissan, The stability of viscous flow between horizontal concentric cylinders, Proc. R. Soc. London A251 (1959) 76.
[16] E.M. Sparrow, On the onset of flow instability in a curved channel of arbitrary height, Z. Angew. Math. Phys. 15 (1964) 638.

[17] J. Walowit, S. Tsao, R. Diprima, Stability of flow between arbitrarily spaced concentric cylindrical surfaces including the effect of a radial temperature gradient, Trans. ASMEE. J. Appl. Mech. 31 (1964) 585.
[18] G.P. Agarwal, Analysis of proteins transmission in vortex flow ultrafilter for mass transfer coefficient, J. Membr. Sci. 136 (1997) 141.
[19] W.S. Opong, A.L. Zydney, Diffusive and convective protein transport through asymmetric membranes, AIChE 37 (10) (1991) 1497.
[20] G.B. van den Berg, I.G. Racz, C.A. Smolders, Mass transfer coefficients in cross-flow ultrafiltration, J. Membr. Sci. 47 (1989) 25.
[21] U.B. Holeschovsky, C.L. Cooney, Quantitative description of ultrafiltration in a rotating filtration device, AIChE J. 37 (1991) 1219.
[22] P. Pradanos, J.I. Arribas, A. Hernandez, Retention of proteins in cross flow UF through asymmetric inorganic membranes, AIChE J. 40 (1994) 190.
[23] W.F. Blatt, A. Dravid, A.S. Michaeles, L. Nelsen, Solute polarization and cake formation in membrane ultrafiltration: causes, consequences and control techniques, in: J.E. Flinn (Ed.), Membrane Science and Technology, Plenum Press, New York, 1970, p.47.
[24] Y. Mori, W. Nakayama, Study on forced convective heat transfer in curved pipes, Int. J. Heat Mass Trans. 8 (1965) 67.
[25] Y. Mori, W. Nakayama, Study on forced convective heat transfer in curved pipes, Int. J. Heat Mass Trans. 10 (1967) 681.
[26] A.N. Dravid, K.A. Smith, E.W. Merrill, P.L.T. Brian, Effect of secondary fluid motion on laminar flow heat transfer in helically coiled tubes, AIChE J. 17 (1971) 1114.
[27] M.A. Lèvèque, Lespois de la transmission de chaleur par convection, Ann. Mines 201 (1928) 305.
[28] G. Jonsson, C.E. Boesen, Polarization phenomenon in membrane processes, in: G. Belfort (Ed.), Synthetic Membrane Processes, Academic Press, New York, 1984, pp. 101–130.
[29] E.L. Cussler, Diffusion Mass Transfer in Fluid systems, Cambridge University Press, Cambridge, 1984.
[30] V. Gekas, B. Hallstrom, Mass transfer in the membrane concentration polarization layer under turbulent cross flow. I: Critical literature review and adaptation of existing Sherwood correlations to membrane operations, J. Membr. Sci. 30 (1987) 153.